# Understanding stress gradients in microelectronic metallization

Conal E. Murray,[1,a)] E. Todd Ryan,[2] Paul R. Besser,[3] Christian Witt,[4] Jean L. Jordan-Sweet,[1] and Michael F. Toney[5]
[1]*IBM T.J. Watson Research Center, Yorktown Heights, New York*
[2]*GLOBALFOUNDRIES, Albany Nanotech Center, Albany, New York*
[3]*GLOBALFOUNDRIES, Sunnyvale, California*
[4]*GLOBALFOUNDRIES, T.J. Watson Research Center, Yorktown Heights, New York*
[5]*Stanford Synchrotron Radiation Lightsource, Menlo Park, California*

(Received 27 January 2012; accepted 31 January 2012)

The manufacture of ultra-large scale integration technology can impose significant strain within the constituent metallization because of the mismatch in coefficients of thermal expansion between metallization and its surrounding environment. The resulting stress distributions can be large enough to induce voiding within Cu-based metallization, a key reliability issue that must be addressed. The interface between the Cu and overlying capping layers is a critical location associated with void formation. By combining conventional and glancing-incidence X-ray diffraction, depth-dependent stress distributions that develop in Cu films and patterned features are investigated. *In situ* annealing and as-deposited measurements reveal that strain gradients are created in capped Cu structures, where an increased in-plane tensile stress is generated near the Cu/cap interface. The interplay between plasticity in Cu and the constraint imposed by capping layers dictates the extent of the observed gradients. Cu films possessing caps deposited at temperatures where Cu experienced only elastic deformation did not exhibit depth-dependent stress distributions. However, all capped Cu samples exposed to temperatures that induce plastic behavior developed greater tensile stress at the Cu/cap interface than in the bulk Cu film after cooling, representing a clear concern for the mitigation of metallization voiding. © *International Centre for Diffraction Data* [doi:10.1017/S0885715612000231]

Key words: X-ray diffraction, microelectronics, copper, stress

## I. INTRODUCTION

The fabrication of Cu-based metallization, which provides power to over a billion transistors associated with current microelectronic processor technology, involves numerous thermal excursions associated with the deposition and subsequent curing of constituent materials that comprise the back end of line. The coefficient of thermal expansion (CTE) mismatch between Cu and the underlying Si substrate can induce significant tensile stress in the metallization after such thermal cycling. Interconnect structures currently include Ta-based barrier layers along both trench bottoms and sidewalls and capping layers on the top surface to limit interdiffusion between Cu and its environment as well as diffusion of Cu along the metallization interfaces. This diffusion, typically caused by either electromigration or stress migration, can be severe enough to induce voiding within interconnect structures, leading to failure of the circuitry. As device dimensions continue to decrease, causing current densities within metallization to increase, the critical void size required to cause failure also decreases with the cross-sectional area of the interconnect structure (Hu *et al.*, 2004).

As electromigration is an activated process, reducing the operating temperature of the interconnect structures helps to decrease electromigration-induced mass flow. However, the phenomena of stress-induced voiding is generally considered a combination of atomic diffusion, which is more pervasive at elevated temperatures, and the magnitude of tensile stress in metallization, which is larger at lower temperatures (Gambino *et al.*, 2009). Therefore, interconnect structures can be most susceptible to stress-induced voiding within an intermediate temperature range. For both failure modes, tensile stress in the Cu features can facilitate the creation of voids. The presence of passivation layers above blanket Cu films has been shown to reduce stress relaxation at higher temperatures (Vinci *et al.*, 1995) by limiting diffusional mechanisms (Keller *et al.*, 1998). As the interface between Cu metallization and capping layers represents a location that is susceptible to electromigration (Hu *et al.*, 2004), a decrease in the relaxation of tensile stress in this region represents a key reliability issue that must be understood.

Glancing-incidence X-ray diffraction (GIXRD) is an important technique to probe strain gradients within a variety of thin-film structures. By choosing the appropriate conditions for the incident and diffracted-beam angles with respect to the film surface, the depth to which the diffraction information is collected can be reduced to tens of nanometers near the critical angle (Parratt, 1954). Previous studies of uncapped Cu films using GIXRD have reported lower in-plane stress at the free surface (Himuro and Takayama, 2005), or a small increase (<40 MPa) that may be caused by surface oxidation (Takayama *et al.*, 2004). Because capping layers are necessary to mitigate oxidation and diffusion at the top surface of

[a)]Author to whom correspondence should be addressed. Electronic mail: conal@us.ibm.com

interconnect metallization, their impact on the mechanical behavior of Cu films must be understood, particularly during subsequent manufacturing steps that involve high temperatures.

## II. EXPERIMENTAL

Ta/TaN barrier layers (30/10 nm thick) and Cu seed layers (80 nm thick) were sputter deposited onto Si (001) wafer substrates (300 mm diameter). Cu films were electroplated onto the Cu seed layers, followed by annealing at 100 °C for 30 min in an inert atmosphere to promote grain growth. After chemical mechanical polishing, the final thickness of the Cu films was approximately 650 nm. One of three types of capping schemes was applied to each wafer: a 35-nm-thick $SiC_xN_yH_z$ film deposited at 350 °C, an electrolessly deposited 7.5-nm CoWP film, or a hybrid cap, consisting of a 7.5-nm CoWP film followed by a 35-nm-thick $SiC_xN_yH_z$ film deposited at 350 °C. Although normal processing conditions produce an in-plane compressive stress in the $SiC_xN_yH_z$ film, the $SiC_xN_yH_z$ cap for one of the wafers was treated in a different manner that produced a residual tensile stress. For the patterned Cu features under investigation, 2-mm-long trenches were etched into a low-k dielectric organosilicate film above $SiC_xN_yH_z/SiO_2$ layers deposited on a 300-mm-diameter Si (001) substrate. The conventional barrier layer and the Cu seed layers were sputter deposited, followed by Cu electroplating and chemical mechanical polishing, to produce Cu lines with thicknesses of approximately 140 nm. The final Cu interconnect stack was capped with a 50-nm $SiC_xN_yH_z$ layer, also deposited at 350 °C. To investigate the effects of subsequent thermal excursions, CoWP-capped Cu films were annealed at 350 °C with a ramp rate of approximately 5 °C/s, using He gas of ultra-high purity (99.999%).

X-ray diffraction measurements of the capped Cu films and features were conducted at Brookhaven National Laboratory's National Synchrotron Light Source X20A beamline (Murray *et al.*, 2008). As shown in Figure 1, diffractive optics in front of the avalanche photodiode detector consisted of a single-bounce Ge (111) analyzer crystal in non-dispersive configuration. X-ray diffraction was used to determine the bulk stress of the Cu films by measuring the appropriate Cu interplanar spacing, $d_{hkl}$, as a function of $\psi$, the angle between the diffraction vector, $k$, and the surface normal, $\hat{n}$, as depicted in Figure 1(a). The sample was tilted about $\psi$ so that the incident and diffracted X-ray beams maintained a symmetric path through the Cu films. Gaussian fits of the Cu (220), (222), or (422) diffraction peak centers were converted into values of $d$ using Bragg's law.

For the in-plane GIXRD measurements (Figure 1(b)), the angles between the incident beam and the sample surface, $\alpha_i$, and between the diffracted beam and sample surface, $\alpha_f$, were kept equal. This symmetric diffraction condition is required so that corrections attributable to refraction of the X-ray beam are negligibly small (Toney and Brennan, 1989; Schute and Cohen, 1991). GIXRD measurements performed using an asymmetric configuration can generate significant shifts in the measured diffraction angle, creating significant error in the corresponding strain measurements without correction (Toney and Brennan, 1989). Cu (220) and Cu (422) reflections, whose normals are perpendicular to [111], were used because the majority of the Cu grains were (111)-oriented. Measurements were conducted in reciprocal space (*hkl*),

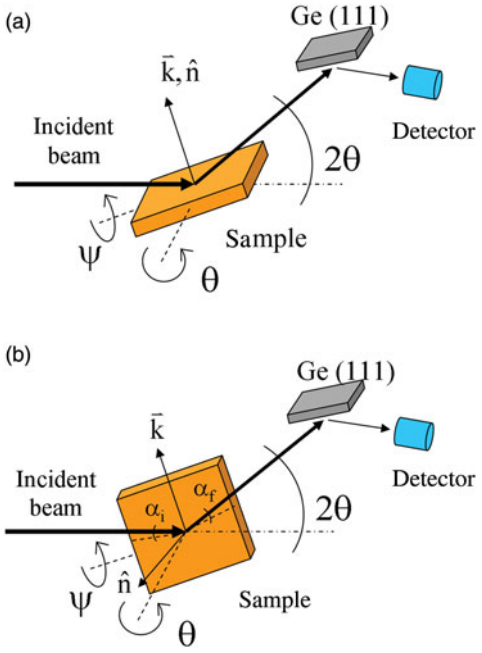


Figure 1. (Color online) X-ray diffraction stress measurements in (a) conventional mode and (b) glancing-incidence geometry.

where diffraction peaks were collected along the in-plane reciprocal lattice vector $h$ for various incidence angles in the range 0.2–2.6°. In glancing incidence, only an evanescent wave penetrates into the film below the critical angle, above which the penetration depth increases rapidly as the incidence angle is increased. Although the critical angle for a Cu film is approximately 0.37° for 8.6 keV photons, the presence of capping layers, which possess different scattering factors from those of Cu, modifies this angle so that the exact penetration depth of the X-rays will differ from that calculated for a single Cu film. The finite horizontal divergence of the X-ray beam as it impinges on the sample also impacts the incidence angle at which diffraction information from the Cu film can be detected.

*In situ* X-ray diffraction measurements were conducted at the Stanford Synchrotron Radiation Lighsource beamline 7-2 where a photon energy of 10.5 keV was used ($\lambda = 1.1808$ Å) (Murray *et al.*, 2010a). The incident beam was monochromatized with double-bounce Si (111) crystals, where the second (sagittal) crystal horizontally focused the beam to about 0.25 mm. Diffractive optics consisted of a single-bounce Ge (111) analyzer crystal, in non-dispersive configuration with the sample. The angular width of the incident beam at the detector was 0.014° full-width at half-maximum in the diffraction plane. $SiC_xN_yH_z$-capped Cu films were heated in an Anton Paar DHS 900 furnace with a helium ambient. Measurements were first conducted at room temperature and then at several temperatures up to 350 °C and down to room temperature. Conventional X-ray diffraction and GIXRD measurements were conducted using the Cu (422) so that $d_{422}$ values obtained using conventional X-ray diffraction measurements could be directly extrapolated to an in-plane value ($\psi = 90°$) to detect any difference between bulk $d_{422}$ and the values measured at glancing incidence. Reciprocal space measurements were also conducted along $h$ for incidence angles in the range 0.3–1.9°.


https://doi.org/10.1017/S0885715612000231 Published online by Cambridge University Press

The blanket films were assumed to possess an isotropic, biaxial in-plane stress state, so that Eq. (1), which represents a simplified form of the X-ray stress equation, could be used to relate the fitted $d$ vs. $\sin^2(\psi)$ slope to the in-plane biaxial stress, $\sigma_{\text{bulk}}$, for a quasi-isotropic elastic material (Noyan and Cohen, 1987):

$$\frac{\partial d_{hkl}}{\partial \sin^2(\psi)} = d_0\left(\frac{1}{2}S_2\right)\sigma_{\text{bulk}} \tag{1}$$

where $\frac{1}{2}S_2$ is one of the two X-ray elastic constants (XECs) commonly used to describe a quasi-isotropic, polycrystalline ensemble. For an elastically isotropic material, $\frac{1}{2}S_2$ can also be represented by $((1+\nu)/E)$, where $E$ and $\nu$ represent the effective Young's modulus and Poisson's ratio, respectively, of the diffracting grains. XECs were calculated using the Neerfeld–Hill limit, which is an average of the Voigt and Reuss value, where for Cu (222), $\frac{1}{2}S_2 = 7.912$ and $9.743$ $\text{TPa}^{-1}$ for both Cu (220) and Cu (422), respectively. For the blanket film measurements, $d_0$ was assumed to be the value of the intercept of the fitted $d$-spacing line ($\psi = 0^0$).

## III. RESULTS

Plots of the Cu (222) interplanar spacings from the $SiC_xN_yH_z$-capped and the CoWP-capped Cu films measured as a function of $\sin^2(\psi)$ are shown in Figures 2(a) and 2(b), respectively. The measured Cu (222) $d$-spacings exhibit linear behavior with respect to $\sin^2(\psi)$, confirming that the Cu films behave as quasi-isotropic elastic, polycrystalline aggregates in which the out-of-plane stress components are negligible. The values of the bulk in-plane biaxial stress, as calculated using Eq. (1), are ~185 and ~121 MPa for the $SiC_xN_yH_z$-capped and the CoWP-capped Cu films, respectively.

Figure 3(a) depicts the corresponding $d$-spacing of the Cu (220) peak measured at glancing incidence as a function of the incident beam angle from the surface of the $SiC_xN_yH_z$-capped Cu film. A gradient in the Cu lattice spacing is evident at small incidence angles, where a larger in-plane lattice spacing is observed near the top surface of the Cu film relative to that in the bulk. Because GIXRD measurements represent a volume average through the penetration depth where absorption of the X-rays follows an exponential dependence (Parratt, 1954), the depth of the diffracting volume increases rapidly as the incident angle is raised above the critical angle. However, the measured Cu (220) spacing for the sample with a CoWP capping layer only, as shown in Figure 3(b), exhibits no gradient in lattice spacing through the film.

For all samples that possessed a $SiC_xN_yH_z$ capping layer, the Cu (220) in-plane spacing was larger near the top surface of the film. The interplanar spacing decreased as the incidence angle was increased, eventually reaching the average value for the bulk film. Clearly, these bulk Cu lattice spacings varied because of the difference in processing conditions and the corresponding average stress state within the Cu films. The increase in in-plane normal stress associated with $d_{hkl}^{\text{surf}}$, the near-surface lattice spacings measured using GIXRD, can be calculated using Eqs (2) and (3):

$$\sigma_{\text{surf}} = \sigma_{\text{bulk}} + \Delta\varepsilon/\left(\tfrac{1}{2}S_2 + 2S_1\right) \tag{2}$$

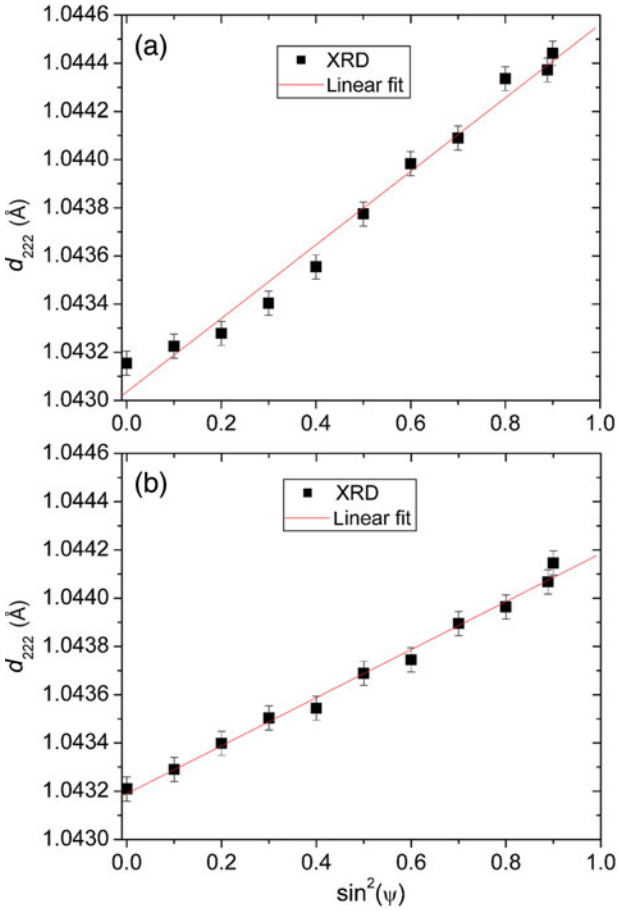


Figure 2. (Color online) Measured Cu (222) reflection peaks vs. $\sin^2(\psi)$ for (a) $SiC_xN_yH_z$-capped Cu film and (b) CoWP-capped film, where $\psi$ is the tilt angle between the surface normal and the diffraction vector.

$$\Delta\varepsilon = \left(\frac{d_{hkl}^{\text{surf}} - d_{hkl}^{\text{bulk}}}{d_{hkl}^{\text{bulk}}}\right) \tag{3}$$

where $S_1$ is the second XEC associated with quasi-isotropic, elastic materials and corresponds to $-\nu/E$. $d_{hkl}^{\text{bulk}}$ corresponds to the value of the lattice spacing as extrapolated from the fit of the conventional X-ray measurements to the in-plane orientation ($\psi = 90°$). The dotted red lines in Figures 3(a) and 3(b) represent the extrapolated lattice spacings, where the values were normalized by the ratio of the root of the sum of the squares of the Miller indices: $d_{220} = d_{222}\sqrt{12/8}$. If we assume that the (111) grains represent the majority texture component in the film, then these grains, which possess (110) and (211) normal to the in-plane direction, would strongly contribute to the glancing-angle diffraction measurements of both Cu (220) and Cu (422) reflections. The XECs in Eq. (2) were calculated in the Neerfeld–Hill limit for (111) grains, where $S_1 = -1.837$ $\text{TPa}^{-1}$ and $\frac{1}{2}S_2 = 7.912$ $\text{TPa}^{-1}$, and the value of $d_{hkl}^{\text{surf}}$ corresponded to measurements conducted at an incidence angle of approximately 0.3°.

The in-plane stress of Cu films as calculated from the $d$ vs. $\sin^2(\psi)$ measurements, corresponding to the bulk film value, and those that include the additional stress in the near-surface regions are shown in Figure 4. A large increase in stress near the top Cu surface, as compared to the bulk, is observed for all of the capping schemes that possess a $SiC_xN_yH_z$ layer.


https://doi.org/10.1017/S0885715612000231 Published online by Cambridge University Press

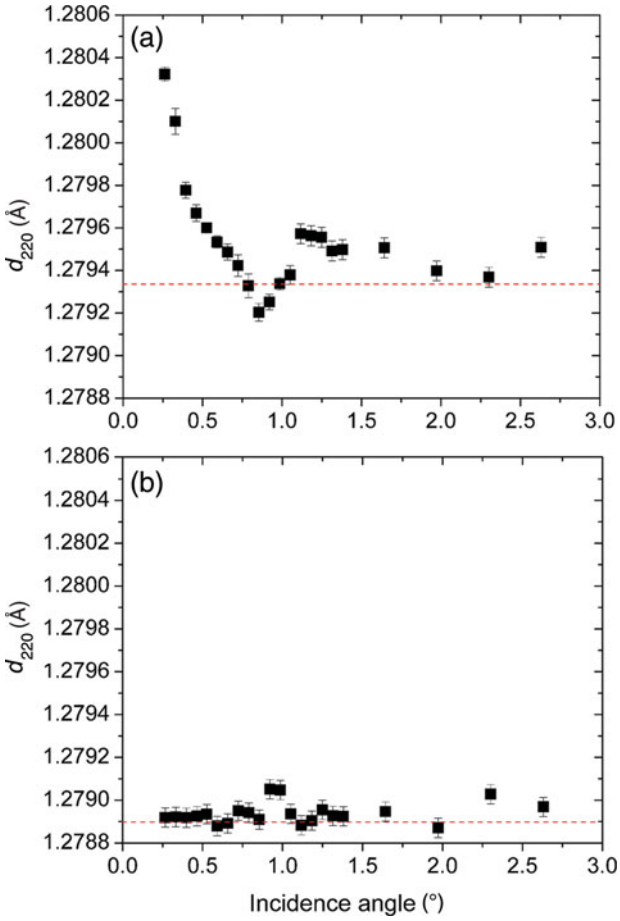


Figure 3. (Color online) Measured Cu (220) reflection peaks vs. incidence angle for (a) $SiC_xN_yH_z$-capped Cu film and (b) CoWP-capped film. The dashed lines refer to extrapolated bulk in-plane values for the $SiC_xN_yH_z$-capped and CoWP-capped Cu films, respectively, as shown in Figure 2.

The greatest increase in tensile stress in the near-surface region was observed in the conventional $SiC_xN_yH_z$-capped Cu film. The stress at the Cu/cap interface for the sample with a tensile $SiC_xN_yH_z$ cap (t-SiCNH) also exhibited a large increase, indicating that the sign of stress in the cap does not significantly impact the observed stress gradients. The sample that possessed only a CoWP cap exhibited a negligible increase in tensile stress near the surface. However, subsequent annealing of the CoWP-capped Cu film (a-CoWP) shows that significant changes were induced in both the bulk stress state and the stress near the Cu/cap interface, where a tensile stress gradient of approximately 107 MPa was introduced. It is interesting to note that this value is similar to that induced by the hybrid capping scheme (117 MPa), where the CoWP layer was in contact with the underlying Cu film. The annealing process doubled the bulk in-plane stress in the CoWP-capped Cu film.

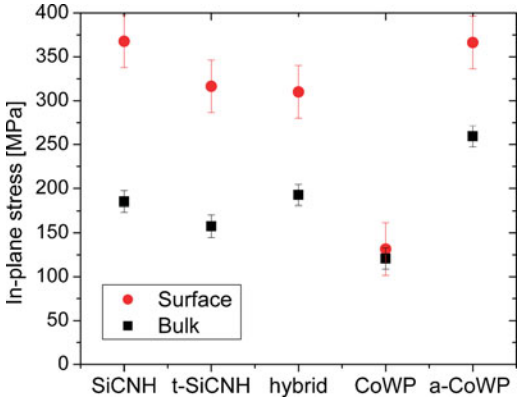


Figure 4. (Color online) Comparison of in-plane stress values in capped Cu films in bulk and near-surface regions for a variety of capping schemes, where "t-SiCNH" refers to a $SiC_xN_yH_z$ cap possessing a residual tensile stress, "hybrid" refers to a CoWP/$SiC_xN_yH_z$ cap and "a-CoWP" refers to a CoWP-capped Cu film exposed to annealing for 5 min at 350 °C.

Figure 5(a) depicts the bulk in-plane stress and the stress near the top surface of the Cu film, as a function of temperature during an *in situ* thermal cycle. A decrease in the stress gradient can be observed as the Cu film temperature is increased from room temperature. At 125 °C, the bulk Cu film exhibits compressive stress, whereas the region near the cap/Cu interface still remains slightly tensile because of the stress gradient. By comparing the evolution of stress to the dashed line, corresponding to linear elastic behavior as a result of CTE mismatch between the Cu and Si substrates, inelastic deformation already occurs in the bulk Cu during the initial stages of heating. However, the Cu film near the cap/Cu interface behaves elastically up to 125 °C, where the presence of the $SiC_xN_yH_z$ cap is expected to constrain Cu diffusion. As the temperature is increased to 350 °C, the stress gradient

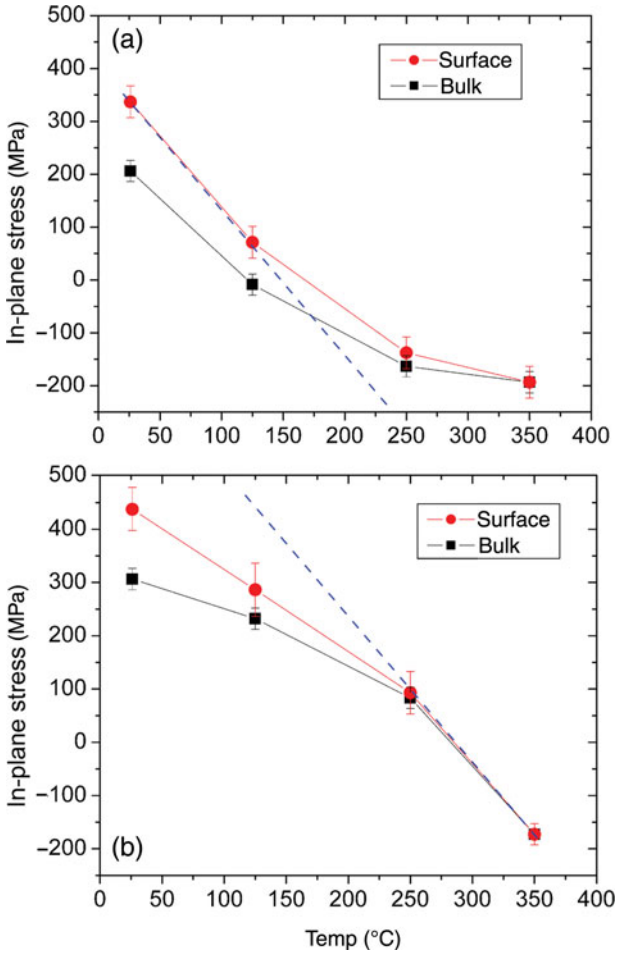


Figure 5. (Color online) In-plane stress measured in the bulk and near-surface regions using Cu (422) reflection of a $SiC_xN_yH_z$-capped Cu film during (a) heating and (b) cooling. The dashed curve, corresponding to stress evolution from elastic CTE mismatch, is included for comparison.


https://doi.org/10.1017/S0885715612000231 Published online by Cambridge University Press

in the Cu film disappears while the bulk Cu stress reaches approximately −190 MPa. Although diffusional creep mechanisms are prevalent at this temperature (Thouless *et al.*, 1993), the stress gradient disappears because the in-plane Cu spacing matches its value during cap deposition at 350 °C. Conventional stress measurements, conducted at 350 °C before and after GIXRD characterization, which took approximately 3 h, revealed that the magnitude of compressive stress in the bulk Cu film decreased by approximately 20 MPa.

Figure 5(b) demonstrates the mechanical response of the capped Cu films during cooling, where the entire Cu film through its thickness exhibited elastic behavior during the initial stages as the CTE mismatch drives the film from compression into tension, resulting in little to no stress gradient in the film. As the film temperature dropped below 250 °C, a difference appeared between the stress state of the near-cap region and that of the bulk Cu. A comparison of the slopes of the stress–temperature curves during cooling indicates that, although the Cu near the capping layer exhibits inelastic behavior, plastic relaxation is more pervasive in the bulk of the film. The bulk stress at room temperature is greater than the initial value attributable to the thermal cycle (Vinci *et al.*, 1995; Keller *et al.*, 1998), whereas the stress gradient in the Cu film is approximately equal before and after the thermal cycle. Cu (220) GIXRD measurements of the patterned Cu features also exhibit a larger in-plane tensile stress both along the lines (longitudinal) and perpendicular to the lines (transverse) near the Cu/cap interface. Extrapolations of the fitted, conventional Cu (220) X-ray stress measurements produced bulk in-plane lattice spacings of 1.280 33 and 1.278 47 Å in the longitudinal and transverse directions, respectively. Because the patterned Cu features possess a triaxial stress state, Eqs. (1)–(3) are inappropriate for converting lattice spacing measurements to in-plane stress values. Tensor multiplication of the stiffness and strain tensors must be used to determine the full stress tensor. If the Cu patterned features can still be considered as elastically quasi-isotropic, then the matrix representation of the multiplication only involves the principal stress and strain components:

$$\begin{Bmatrix} \Delta\varepsilon_{11} \\ \Delta\varepsilon_{22} \\ \Delta\varepsilon_{33} \end{Bmatrix} = \begin{bmatrix} S_1 + \frac{1}{2}S_2 & S_1 & S_1 \\ S_1 & S_1 + \frac{1}{2}S_2 & S_1 \\ S_1 & S_1 & S_1 + \frac{1}{2}S_2 \end{bmatrix} \times \begin{Bmatrix} \Delta\sigma_{11} \\ \Delta\sigma_{22} \\ \Delta\sigma_{33} \end{Bmatrix} \quad (4)$$

where $\Delta\varepsilon_{ij}$ and $\Delta\sigma_{ij}$ refer to the increase in strain and stress near the top Cu surface, respectively. If we assume that the change of out-of-plane stress ($\Delta\sigma_{33}$) is zero near the vicinity of the top Cu surface, then the increase in the in-plane stress values takes the form (Murray *et al.*, 2011b):

$$\begin{Bmatrix} \Delta\sigma_{11} \\ \Delta\sigma_{22} \end{Bmatrix} = \frac{1}{(2S_1 + \frac{1}{2}S_2)\frac{1}{2}S_2} \begin{bmatrix} S_1 + \frac{1}{2}S_2 & -S_1 \\ -S_1 & S_1 + \frac{1}{2}S_2 \end{bmatrix} \times \begin{Bmatrix} \Delta\varepsilon_{11} \\ \Delta\varepsilon_{22} \end{Bmatrix} \quad (5)$$

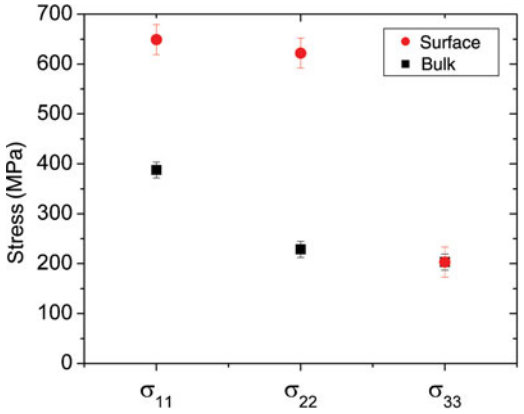


Figure 6. (Color online) Triaxial stress state in 150-nm wide Cu interconnect/low-k dielectric patterned features in bulk and near-surface regions, where $\sigma_{11}$ corresponds to stress along the interconnect, $\sigma_{22}$ to stress transverse to the interconnect, and $\sigma_{33}$ to stress in the out-of-plane direction.

Equation (3) may be applied to determine the increase in the in-plane strain, for which $\Delta\varepsilon_{11} = 8.67 \times 10^{-4}$ and $\Delta\varepsilon_{22} = 19.09 \times 10^{-4}$. By using the elastic constants for Cu (111) calculated in the Neerfeld–Hill limit, the resultant increase in the in-plane stress values are $\Delta\sigma_{11} = 262$ and $\Delta\sigma_{22} = 393$ MPa. These values are added to the bulk, triaxial stress tensor components found in the Cu interconnects (Murray *et al.*, 2011a), measured using a combination of the Dölle–Hauk approach (Dölle and Hauk, 1976) and the least-squares minimization technique of Winholz and Cohen (1988). The resulting in-plane stress values near the top surface of the Cu film, as shown in Figure 6, are almost equal after combining the additional stress induced by the cap. This result suggests that the effects of elastic relaxation caused by the presence of the more compliant low-k dielectric insulation between the Cu lines, which substantially reduces the bulk Cu stress in the direction transverse to the lines ($\sigma_{22}$), has little impact on the stress state of Cu near its top surface. The lack of increase in the out-of-plane stress ($\sigma_{33}$) is simply a consequence of the assumption required to solve for the stresses in Eq. (5).

## IV. DISCUSSION

The initial stress gradient at room temperature found in both the capped Cu films and patterned features originates from a larger in-plane Cu lattice spacing near the capping layer relative to that in the bulk, imposed by the $SiC_xN_yH_z$ cap as the sample cools from the capping layer deposition temperature (Murray et al., 2008, 2010b). $SiC_xN_yH_z$ deposition takes place at elevated temperatures (350 °C) at which significant plastic deformation occurs to partially relieve the compressive stress generated from CTE mismatch. The presence of passivation layers on the top surface of Cu films has been demonstrated to reduce stress relaxation at temperatures above 300 °C (Vinci *et al.*, 1995; Keller *et al.*, 1998), as confirmed by the large residual compressive stress in the bulk Cu film during *in situ* annealing, which only experiences a 20 MPa reduction averaged through the entire thickness of the film. The magnitude of bulk stresses in bare Cu films remains low during the initial portion of the cooling process where


https://doi.org/10.1017/S0885715612000231 Published online by Cambridge University Press

diffusional transport is prevalent (Flinn, 1991; Gan et al., 2006). In contrast, passivated Cu films exhibit both a greater compressive stress at high temperatures and an immediate decrease on cooling that followed a linear trend to tensile stress generated from the CTE mismatch. As shown in Figure 5(b), the slope in this region of the stress–temperature behavior matches that predicted for elastic deformation in Cu (−2.77 MPa/°C), and a stress gradient does not develop immediately upon cooling to 250 °C. This confirms that the cap creates the stress gradient in the underlying Cu at lower temperatures by mitigating the extent of plastic deformation near the cap/Cu interface as the thermal stress increases. On further cooling from the deposition temperature, the CTE mismatch drives the Cu film into tension of sufficient magnitude to activate plastic relaxation and thus the stress gradient is re-established.

The residual stress state of the $SiC_xN_yH_z$ cap appears to play a small role in the increase in stress near the surface of blanket Cu films. The Cu film with a residual tensile $SiC_xN_yH_z$ cap exhibited an increase of 159 MPa, as compared to 182 MPa in the case of a compressively stressed $SiC_xN_yH_z$ capping layer, indicating that the net force of the capping layer is primarily accommodated by the underlying Si substrate. Cu films only experience a small temperature increase during CoWP deposition (80 °C), resulting in predominantly elastic deformation. Exposing these films to the same temperature as that associated with $SiC_xN_yH_z$ deposition induces a larger tensile stress at room temperature, which is expected because of microstructural changes such as grain growth (Flinn, 1991; Vinci *et al.*, 1995; Shen and Ramamurty, 2003). The introduction of a stress gradient in the CoWP-capped Cu films confirms that the capping layer suppresses Cu diffusion near the Cu/cap interface as the sample cools. It is the thermal history and not the composition of the cap that produces the stress gradient, assuming that the capping layer possesses sufficient adhesion to mitigate diffusion in the underlying Cu.

Measurements on the Cu line arrays confirm that stress gradients increase the in-plane tensile stress values in patterned features as well. Although the magnitude of the increase differs between the longitudinal and transverse directions, where the increase in stress perpendicular to the lines is larger by approximately 130 MPa, the bulk transverse stress was measured to be lower than that along the lines because of load sharing with the adjacent low-k dielectric material between the lines. The combined response, as shown in Figure 6, indicates that the stress state at the top surface of the Cu interconnects is approximately equal along its longitudinal and transverse directions. The impact of the overlying capping layer plays a larger role in the mechanical response of the stress near the Cu/cap interface than the more compliant, low-k dielectric film that dictates the bulk Cu stress. However, the presence of stress gradients suggests that determination of the stress state in Cu features using only grazing-incidence values to measure the in-plane unit-cell spacings (Wilson *et al.*, 2009) will not accurately capture the true mechanical behavior of the features.

## V. CONCLUSION

A combination of conventional X-ray diffraction and GIXRD measurements revealed that stress gradients are generated in capped Cu films and features because of the overlying constraint imposed by the cap near the top Cu surface when plastic relaxation mechanisms are active. In-plane stress values near the top surface of Cu films and features were larger than those in the bulk Cu for samples possessing a $SiC_xN_yH_z$ capping layer, which is deposited at 350 °C. Although CoWP-capped Cu films experienced elastic deformation and did not exhibit a stress gradient, subsequent annealing to 350 °C also induced a tensile stress gradient. *In situ* GIXRD measurements conducted during thermal cycling revealed that in-plane stress gradients at the Cu film/$SiC_xN_yH_z$ cap interface decrease as the sample temperature is increased to match that of the cap deposition. The cap constrains diffusional flow along this interface which inhibits relaxation of the bulk Cu compressive stress at 350 °C while the stress gradient is removed. The gradient reappears after the sample is cooled to temperatures below which the magnitude of the thermal stress is sufficient to induce plastic relaxation in the bulk Cu. Thermal excursions to higher temperatures cannot be used to eliminate tensile stress gradients in Cu, leaving the top Cu surface more susceptible to the creation of voids. It should be noted that the use of grazing-incidence measurements to detect in-plane lattice spacings does not produce stress values representative of the bulk.

## ACKNOWLEDGMENTS

This work was performed by the Research Alliance Teams at various IBM Research and Development facilities. Diffraction measurements carried out at the National Synchrotron Light Source, Brookhaven National Laboratory were supported by the U.S. Department of Energy, Division of Materials Sciences and Division of Chemical Sciences. The authors wish to acknowledge Dr Valery Borzenets for assistance with the diffraction measurements carried out at the Stanford Synchrotron Radiation Light source, which is also supported by the U.S. Department of Energy, Division of Materials Sciences and Division of Chemical Sciences.

Dölle, H. and Hauk, V. (**1976**). "Röntgenographische Spannungsermittlung der Eigenspannungssysteme allgemeiner Orientierun," Harterei-Tech. Mitt. **31**, 165–168.

Flinn, P. A. (**1991**). "Measurement and interpretation of stress in copper films as a function of thermal history," J. Mater. Res. **6**, 1498–1501.

Gambino, J. P., Lee, T. C., Chen, F., and Sullivan, T. D. (**2009**). "Reliability of copper interconnects: stress-induced voids," ECS Trans. **18**, 205–211.

Gan, D., Ho, P. S., Pang, Y., Huang, R., Leu, J., Maiz, J., and Scherban, T. (**2006**). "Effect of passivation on stress relaxation in electroplated copper films," J. Mater. Res. **21**, 1512–1518.

Himuro, T. and Takayama, S. (**2005**). "Temperature dependence of stress distribution in depth for Cu thin films," Mat. Res. Soc. Symp. Proc. **854E**, U11.11.

Hu, C-K., Canaperi, D., Chen, S. T., Gignac, L. M., Herbst, B., and Kaldor, S. (**2004**). "Effects of overlayers on electromigration reliability improvement for Cu/low k interconnects", IEEE 42nd International Reliability Physics Symposium, 222–228.

Keller, R-M., Baker, S. P., and Arzt, E. (**1998**). "Quantitative analysis of strengthening mechanisms in thin Cu films: effects of film thickness, grain size and passivation," J. Mater. Res. **13**, 1307–1317.

Murray, C. E., Besser, P. R., Witt, C., and Jordan-Sweet, J. L. (**2008**). "Stress gradients induced in Cu films by capping layers," Appl. Phys. Lett. **93**, 221901.

Murray, C. E., Besser, P. R., Witt, C., and Toney, M. F. (**2010a**). "In situ evolution of stress gradients in Cu films induced by capping layers," Appl. Phys. Lett. **96**, 261903.

Murray, C. E., Besser, P. R., Witt, C., and Jordan-Sweet, J. L. (**2010b**). "Stress gradients observed in Cu thin films induced by capping layers," J. Mater. Res. **25**, 622–628.
Murray, C. E., Besser, P. R., Ryan, E. T., and Jordan-Sweet, J. L. (**2011a**). "Triaxial stress distributions in Cu/low-k dielectric interconnect features," Appl. Phys. Lett. **98**, 061908.
Murray, C. E., Besser, P. R., Ryan, E. T., and Jordan-Sweet, J. L. (**2011b**). "Evolution of stress gradients in Cu films and features induced by capping layers," Microelectronic Eng. (In press).
Noyan, I. C. and Cohen, J. B. (**1987**). *Residual Stress* (Springer-Verlag, New York), 122.
Parratt, L. G. (**1954**). "Surface studies of solids by total reflection of X-rays," Phys. Rev. **95**, 359–369.
Schute, C. J. and Cohen, J. B. (**1991**). "Strain gradients in Al-2% Cu thin films," J. Appl. Phys. **70**, 2104–2110.
Shen, Y-L. and Ramamurty, U. (**2003**). "Temperature-dependent inelastic response of passivated copper films: experiments, analyses and implications," J. Vac. Sci. Tech. B. **21**, 1258–1264.
Takayama, S., Oikawa, M., and Himuro, T. (**2004**). "Thermal stability and internal stress for strongly (111) oriented Cu films," Mat. Res. Soc. Symp. Proc. **795**, U5.11.
Thouless, M. D., Gupta, J., and Harper, J. M. E. (**1993**). "Stress development and relaxation in copper films during thermal cycling," J. Mater. Res. **8**, 1845–1852.
Toney, M. F. and Brennan, S. (**1989**). "Observation of the effect of refraction on x rays diffracted in a grazing-incidence asymmetric Bragg geometry," Phys. Rev. B, **39**, 7963–7966.
Vinci, R. P., Zielinski, E. M., and Bravman, J. C. (**1995**). "Thermal strain and stress in copper thin films," Thin Solid Films, **262**, 142–153.
Wilson, C. J., Croes, K., Zhao, C., Metzger, T. H., Zhao, L., Beyer, G. P., Horsfall, A. B., O'Neill, A. G., and Tokei, Z. (**2009**). "Synchrotron measurement of the effect of linewidth scaling on stress in advanced Cu/low k interconnects," J. Appl. Phys. **106**, 053524.
Winholz, R. A. and Cohen, J. B. (**1988**). "Generalised least-squares determination of triaxial stress states by X-ray diffraction and the associated errors," Aust. J. Phys. **41**, 189–199.


https://doi.org/10.1017/S0885715612000231 Published online by Cambridge University Press